Evolving Plastic Neural Controllers stabilized by Homeostatic Mechanisms for Adaptation to a Perturbation

Thierry Hoinville and Patrick Hénaff
LIRIS-UVSQ-CNRS, 10-12, avenue de l'Europe, 78140 VÉLIZY, FRANCE
thierry.hoinville@liris.uvsq.fr

Abstract

This paper introduces our ongoing work consisting of evolving bio-inspired plastic neural controllers for autonomous robots submitted to various internal and external perturbations: transmission breaking, slippage, leg loss, etc. We propose a classical neuronal model using adaptive synapses and extended with two bio-inspired homeostatic mechanisms. We perform a comparative study of the impact of the two homeostatic mechanisms on the evolvability of a neural network controlling a single-legged robot that slides on a rail and that is confronted to an external perturbation. The robot has to achieve a required speed goal given by an operator. Evolved neural controllers are tested on long-term simulations to statistically analyse their stability and adaptivity to the perturbation. Finally, we perform behavioral tests to verify our results on the robot controlled with a sinusoidal input while a perturbation occurs. Results show that homeostatic mechanisms increase evolvability, stability and adaptivity of those controllers.

Introduction

Evolving neural controllers to control autonomous robots has been successfully applied to various problems (Meyer et al., 2002; Ijspeert et al., 1998; Nolfi, 1997; Gallagher et al., 1996). However, the majority of the proposed methods produces solutions that are efficient in constant environmental conditions. Recently, evolutionary robotics raise the issue of attempting to build fault-tolerant controllers *adaptive* to internal and environmental *perturbations* (Floreano and Urzelai, 2000; Dittrich et al., 1998). The IRON[1] project, is intended to increase the autonomy and the robustness of robots by confronting evolutionary adjusted neural controllers with different kinds of perturbations: transmission breaking, adherence losses, leg loss, material wear, *etc.* A promising way to do this is to incorporate into neural controllers some plasticity mechanisms inspired by biology (Floreano and Urzelai, 2000). Nevertheless, this plasticity might not be sufficient because it tends to *destabilize* those controllers.

In this paper, we will perform a *comparative* study of effects of two bio-inspired homeostatic mechanisms on the evolvability of plastic neural controllers embodied in a single-legged robot. Subsequently, we will analyse control stability and its adaptivity to an *external* perturbation.

The paper is organized as follows: the first section briefly presents two homeostatic mechanisms from a biological point of view, the second is devoted to the formalization of these mechanisms in our neural model and its application to make a controller for a simulated robot in an evolutionary way. The third section shows statistical and behavioral results, after which results and mechanism modelling are discussed. In the final section, we conclude by giving further developments within our project.

Homeostatic mechanisms in biological neurons

Historically, research in neurophysiology initially centered on synaptic plasticity (Hebb, 1949). The mechanisms controlling this plasticity are commonly considered as the main vector of information storage in neural networks and synaptic connection refinement during cerebral development. Thus, by establishing correlation between simultaneous active neurons, Hebbian rules allow neural circuits to adapt to received information. Nevertheless, these flexibility mechanisms are sources of instability (Miller and MacKay, 1994). Recent studies (Turrigiano, 1999), show that they are associated with homeostatic rules which regulate intrinsic properties of each neuron. In this paper, we are interested in two kinds of these: one regulating neuronal excitability and the other stabilizing total synaptic input strength of each neuron.

Regulation of excitability

Excitability of a neuron, i.e. its propensity to transmit action potentials according to information it gets, depends on concentrations of various molecules which are present in its cell body and in its close vicinity. Ion channels inserted in its membrane *actively* regulate these concentrations. Accord-

[1] Implémentation RObotique de Neuro-contrôleurs adaptatifs (http://www.liris.uvsq.fr/iron/Iron.html). This project, initiated by J.-A. Meyer from the AnimatLab, is supported by the ROBEA program of the CNRS (http://www.laas.fr/robea).

ing to (Desai et al., 1999), this regulation seems to be driven by the average activity of the cell. Thus, when activity of a neuron is high, its excitability decreases to return to a functional firing rate. Conversely, if the cell tends to be silent, its excitability increases until its firing rate gets back to a functional range (top of figure 1).

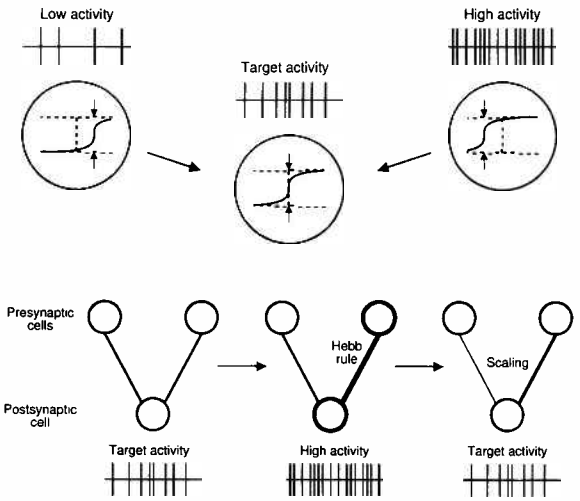

Figure 1: Two homeostatic mechanisms regulating intrinsic properties of neurons. Circles represents nerve cells. (These figures are directly inspired from (Turrigiano, 1999)) Top: Regulation of excitability. The cell's activation threshold is regulated according to its own activity. Bottom: Multiplicative scaling of all synaptic inputs strengths. After an hebbian potentiation of a synapse, the scaling mechanism induces synaptic competition on postsynaptic cell's inputs. Bold circles symbolize activated neurons. Line widths indicates the strength of the corresponding connection.

Stabilization of total synaptic strength

During development and learning, the number of synapses and their properties are submitted to marked changes. These modifications can severely alter activity patterns of neurons. According to (Turrigiano et al., 1998), to preserve their functionalities, neurons regulate their total synaptic input strength. Thus, the excitation amplitude remains in a relevant domain (bottom of figure 1). Experimental observations tend to indicate that this regulation is applied *multiplicatively* and globally to all synaptic inputs of a related cell. By its multiplicative nature, this mechanism ensures relative weights of the different connections. Furthermore, far from neutralizing individual synaptic plasticity, this process induces *competition*: if some connections are potentiated, the strengths of the others must decrease.

Methods

Neuron and synapse model

In the following, we propose extensions to a classical neural model that implement the two homeostatic mechanisms presented above. The extensions can be turned on or off, independently of each other, so it allows comparative study of these mechanisms. It should be noted that these mechanisms, naturally dynamic and activity-dependent, are formalized here in a *static* way. Since the time constant of these mechanisms is much higher than those of the activation and learning processes, we assume this is an acceptable simplification.

Classical model (CM) Nerve cells composing our neural controller are based on a *leaky integrator* model (Beer, 1995):

$$\tau_i^* \frac{dy_i}{dt} = -y_i + \frac{1}{N_i}\sum_{j=1}^{N_i} w_{ij} o_j + I_i \quad (1)$$

$$o_i = \frac{1}{1+e^{-\alpha_i(y_i-\theta_i)}} \quad (2)$$

where y_i represents the mean membrane potential of the neuron i and o_i its activity. w_{ij} is the synaptic strength of the connection from neuron j to neuron i, N_i is the number of synaptic inputs of the neuron i and τ_i^* denotes the time constant of the membrane potential. I_i corresponds, in the case where the cell i is a sensory neuron, to an external excitation coming from a sensor. Finally, α_i is a gain determining the slope of the sigmoidal activation function and θ_i is the threshold of the neuron's activity.

As we want to study neural controllers with intrinsic plasticity, we use the *adaptive synapses* model taken from (Floreano and Urzelai, 1999) in which one local adaptation rule among four is assigned to each connection, as suggested by biological observations. The synaptic weights are updated at each sensory-motor cycle according to the following expression:

$$\widetilde{w}_{ij}^{t+\Delta t} = \widetilde{w}_{ij}^{t} + \frac{\Delta t}{\tau_{ij}^{\odot}} \Delta \widetilde{w}_{ij} \quad (3)$$

where $\widetilde{w}_{ij}$ means $|w_{ij}|$, $\tau_{ij}^{\odot}$ is the time constant of the adaptation rule (comparable to the learning rate, η, in the Floreano's model) and $\Delta\widetilde{w}_{ij}$ is one of the four adaptation rules:

Plain Hebb rule

$$\Delta \widetilde{w}_{ij} = (1-\widetilde{w}_{ij}) o_j o_i \quad (4)$$

Pre-synaptic rule

$$\Delta \widetilde{w}_{ij} = (1-\widetilde{w}_{ij}) o_j o_i + \widetilde{w}_{ij} o_j (o_i - 1) \quad (5)$$

Post-synaptic rule

$$\Delta\widetilde{w}_{ij} = (1-\widetilde{w}_{ij})o_j o_i + \widetilde{w}_{ij}(o_j-1)o_i \tag{6}$$

Covariance rule

$$\Delta\widetilde{w}_{ij} = \begin{cases} (1-\widetilde{w}_{ij})\delta(o_j,o_i) & \text{if } \delta(o_j,o_i) > 0 \\ \widetilde{w}_{ij}\delta(o_j,o_i) & \text{otherwise} \end{cases} \tag{7}$$

where $\delta(o_j,o_i) = \tanh(4(1-|o_j-o_i|)-2)$ is a measure of the difference between o_j and o_i. Note that, in this model, values of synaptic weights are constrained in the interval [-1,1].

Center-crossing mechanism (CC) In order to model the mechanism that regulates neuronal excitability, we use the model of *center-crossing neural networks* proposed in (Mathayomchan and Beer, 2002). This paradigm consists of determining the ideal activation threshold of a neuron according to its synaptic input weights.

$$\theta_i = \frac{1}{2}\sum_{j=1}^{N_i} w_{ij} \tag{8}$$

In this way, the operating range of each neuron is centered about the most sensitive region of its activation function. Indeed, due to the sigmoid asymmetry (about the x-axis), the excitation range of a neuron can be shifted according to the weight values of its synaptic inputs. Formally, this concept can be reduced to the use of a symmetric activation function like the hyperbolic tangent. In our model, we don't use eq. (8) to replace θ_i in eq. (2) but we adapt it according to the following expression:

$$\tau_i^* \frac{dy_i}{dt} = -y_i + \frac{1}{N_i}\sum_{j=1}^{N_i} w_{ij}(2o_j - 1) + I_i \tag{9}$$

Thus, we preserve the same parameterization between the CM and the CC models. Also, the difference of the CC model is that the activation threshold of a neuron becomes totally independent of its synaptic input strengths.

Normalization of synapses mechanism (NS) On the other hand, the mechanism that regulates total synaptic input strengths is modeled by a multiplicative normalization of $\|\vec{w}_i\| = \sqrt{\sum_{j=1}^{N_i} {w_{ij}}^2}$ (Gerstner and Kistler, 2002). To implement this mechanism, eq. (1) and eq. (3) are altered as follows:

$$\tau_i^* \frac{dy_i}{dt} = -y_i + \frac{1}{\sqrt{N_i}}\sum_{j=1}^{N_i} w_{ij}o_j + I_i \tag{10}$$

$$\widetilde{w}_{ij}^{t+\Delta t} = \frac{\widetilde{w}_{ij}^{t} + \frac{\Delta t}{\tau_{ij}^{\odot}}\Delta\widetilde{w}_{ij}}{\sqrt{\sum_{j=1}^{N_i}\left(\widetilde{w}_{ij}^{t} + \frac{\Delta t}{\tau_{ij}^{\odot}}\Delta\widetilde{w}_{ij}\right)^2}} \tag{11}$$

Finally, the above extensions allows the instantiation of four models:

- *center-crossing* model with normalized synapses (CCNS),
- *center-crossing* model (CC),
- normalized synapses model (NS),
- classical model (CM).

Application problem

The aim of the IRON project is to provide a *multi-legged* robot with a neuro-controller, synthesized by evolution, that can adapt its behavior to perturbations. These perturbations can be external (environmental changes) or internal (mechanical or electrical faults). However, a main issue of evolutionary robotics, called the *scalability* problem, is the application of its methods to systems that show a high degree of complexity. Also, to compare the four neural models described before, we apply our approach to a single-legged robot simulation[2].

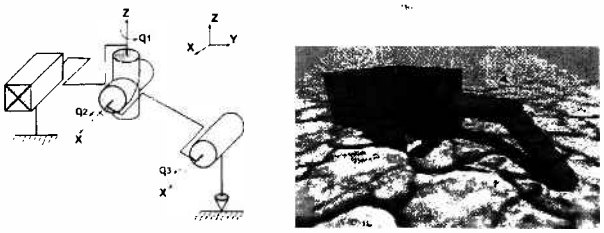

Figure 2: Morphology of the single-legged robot. Left: Kinematic model. Right: Simulation view.

The robot (figure 2) is composed of a body and a leg endowed with three degrees of freedom: two for the hip and one for the knee (see table 1 for mass and geometrical parameters). A binary contact sensor is fixed on the leg tip and on each joint, a servo-motor ordering its angular position is simulated.

[2]Based on a simulator called Open Dynamic Engine (`http://q12.org/ode/`).

Part	Shape	Mass [kg]	Dimension [cm]
body	box	3	20×20×10
hip	sphere	0.5	∅8
thigh	capped cylinder	0.5	15×∅4
shank			

Table 1: Mechanical parameters of the robot

A prismatic link connecting the robot body to the ground, constrains its movements by guiding it on $\vec{X}$ axis. A viscous friction force is applied to the robot. This force F_{fr} is equal to $-k_{fr}V_{eff}$ where V_{eff} is the effective speed of the robot body's centre of mass and k_{fr} is the viscous coefficient.

The task of the robot is to respect a desired walking speed V_{des} and to simultaneously offset a potential perturbation consisting of varying the coefficent k_{fr}. This perturbation, external from the leg's point of view, could simulate, from a multi-legged robot's point of view, an internal perturbation as a mass growth or a disruption of another leg.

The performance p, of a controller is evaluated at the end of a simulation of $T = 10$ sec. according to the following expression:

$$p = \frac{1}{T}\int_0^T |V_{des} - \widetilde{V_{eff}}|dt$$

where $\widetilde{V_{eff}}$ is the global walking speed of the robot[3].

During evolution, each controller is evaluated through three successive simulations with different scenarios. As we can see on table 2, a scenario is defined by temporal variations of V_{des} and k_{fr} parameters. The scenario A corresponds to a simple control behavior, the scenario B rewards the capacity of inhibiting robot gait and the scenario C favours adaptation to the perturbation.

	Scenario A	Scenario B	Scenario C
V_{des}		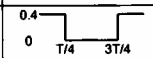	0.3
k_{fr}	10	10	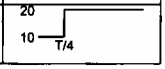

Table 2: Three evaluation scenarios

The global fitness of an individual is the quadratic combination of the three elementary scores obtained from these evaluations (the lower the fitness is, the better the controller behaves).

$$fitness = \sqrt{{p_A}^2 + {p_B}^2 + {p_C}^2}$$

This kind of combination restricts the compensation effect produced by a classical average and supports behaviors that include the three qualities described by the scenarios.

[3]Temporal average calculed by application of a second order low-pass filter on V_{eff}. This value is preferred to V_{eff}, subject to high amplitude variations at the time of each stride.

Neural controller structure and genetic encoding scheme

Figure 3 represents an example of an evolved controller. We arbitrarily fix the network size to eight neurons. Two neurons receive sensorial information from the environment, the first one is excited with the consign error $V_{des} - V_{eff}$, the second one is connected to the contact sensor. Three motoneurons drive angular positions of servomotors. The three remaining neurons form the hidden layer of the network.

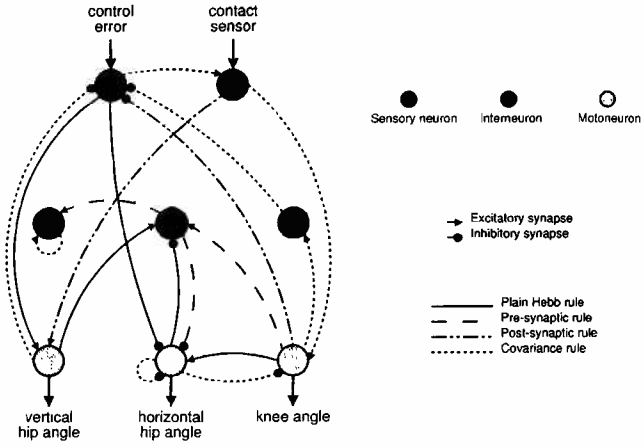

Figure 3: Example of the phenotype structure of an evolved controller.

Controllers are genetically encoded with numerical and symbolic alleles strings divided in eight neuronal blocks. Figure 4 shows structure of the neuron genotype. A neuronal block is composed of a list of intrinsic neuronal parameters ($\tau^\star$, α et θ) and a list of eight synaptic blocks defining properties of cell's output connections with others neurons (including itself). The first synaptic block gene condition the network structure by activating or not the related connection. The next gene indicates its excitatory or inhibitory mode. The two remaining genes dictate the connection dynamic by associating to it one of the four learning rules showed above and the related time constant, $\tau^{\odot}$. The value of each numerical gene is taken from a five length allele set. Table 3 shows these allele sets.

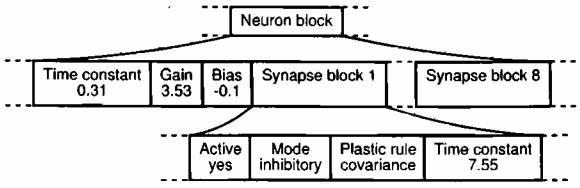

Figure 4: Structure of the neuron genotype.

From a complexity point of view, each genotype is provided with $8 \times (3 + 8 \times 4) = 280$ genes and the size of the

Gene	Alleles set				
$\tau^{\star}$	0.02,	0.165,	0.31,	0.455,	0.6
α	2.46,	3.53,	5.34,	9.43,	31.26
θ	-0.2,	-0.1,	0,	0.1,	0.2
$\tau^{\odot}$	0.2,	2.65,	5.1,	7.55,	10

Table 3: Alleles sets of numerical genes

genotype search space is $\left(5 \times 5 \times 5 \times (2 \times 2 \times 4 \times 5)^8\right)^8 = 3.74 \times 10^{138}$ possibilities.

Controllers are evolved by a generational and elitist genetic algorithm. Genetic operators are the allelic mutation ($P_{mut} = 0.001$) and the uniform crossover ($P_{cross} = 0.6$). Individuals are selected by the stochastic universal sampling algorithm (Baker, 1987) according linearly to their rank in the population (Goldberg, 1989) (with the best individual producing an average 1.1 offspring).

Results

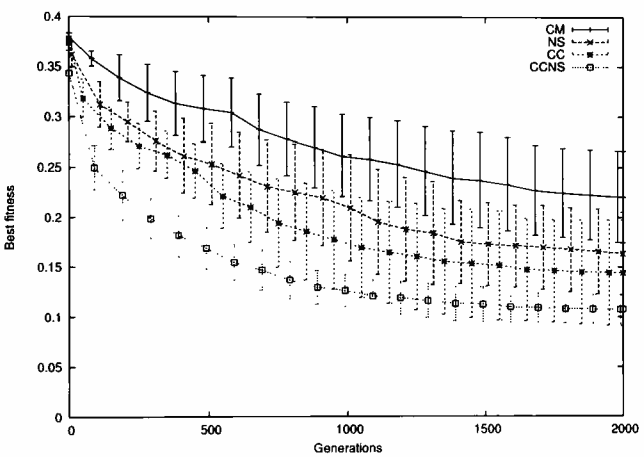

Figure 5: Best fitness for each neural model averaged over 10 runs with different random initializations of the population.

For each neuronal models, we performed 10 evolution runs with different random initializations of populations of 200 individuals. Populations are evolved during 2000 generations. Figure 5 shows statistical results of this experiment in term of best fitness. From these data, four main results can be observed:

- Both homeostatic mechanisms (CC and NS) clearly improve evolvability of the controllers, either in final solution or in evolution speed.
- With the CC controller model, results of evolutionary process strongly depends on the initial random population.
- The NS model is, on average, less effective than the CC model but the standard deviation of the results in the NS case is smaller than in the CC case.
- The CCNS model has the best performance and always results in efficient controllers.

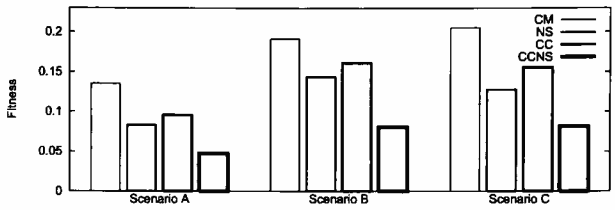

Figure 6: Average fitness of the best controllers (one from each evolution run), according to a scenario and a neural model. Fitness are evaluated during a simulation of 100 sec.

To verify relevance of these results, we evaluated, for each neuronal model and scenario, average fitness of the 10 best controllers taken from the above 10 evolution runs. To test long-term stability of these controllers, each is evaluated during a $T = 100$ sec. simulation. Resulting data are presented on Figure 6. These results corroborate our previous observations except for relative performances of the CC and NS models. This point will be discussed in the next section.

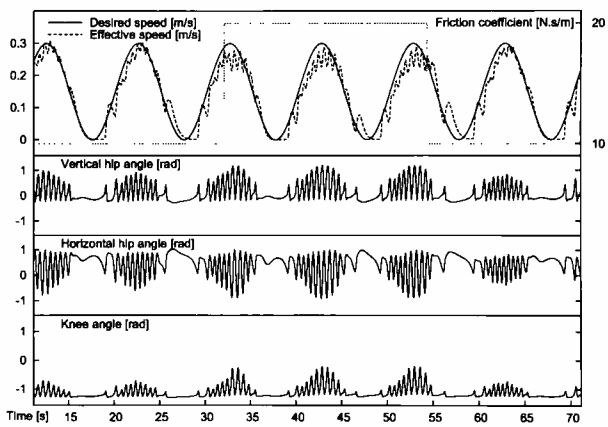

Figure 7: Time-plots of V_{des}, $\widetilde{V_{eff}}$, k_{fr} and joint commands for a CCSN controller. The robot is perturbated from $t = 32$ sec during about 22 sec. Robot strides cause light oscillations of $\widetilde{V_{eff}}$ (attenuated by the low-pass filter).

As a final step, we did a behavioral analysis of the best controllers. During this experiment, a sinusoidal desired speed is indicated to the robot while a perturbation occurs. Figure 7 shows an example of time-plots obtained for a simulation of a CCNS controller. Friction coefficient and joint commands given by the neural network ouputs are also plotted. From these plots, we can see that the control task is

satisfied even when the perturbation occurs. Indeed, in the case of a non-adaptive controller, an increase of 100% of the viscous friction coefficient should cause decrease of 50% of its speed. Yet, figure 7 shows that the perturbation does not significantly alter the robot gait, the control task error remaining relatively small. Moreover, perturbation adaptation is confirmed by time-plots of joint commands. Increasing of the friction force causes amplification of signals send to servo-motors (particularly obvious on the knee joint). Note that walking frequency is not altered by the perturbation.

Discussion

As the above results show, when simulation time is increased, NS controllers are more efficient than CC controllers. By analysing long-term behavior of both models, it can be seen that normalized synapses contribute to stabilizing neural network function. Indeed, CC and CM controllers produce less robust oscillatory patterns. Preliminary obervations indicate that these neural networks cannot reconfigure their synaptic strengths after an inhibition or a perturbation of the robot gait. We suppose that the synaptic normalization constraint favours dynamical stability of neuronal systems. Also, this could explain the low standard deviation of NS and CCNS evolution results (figure 5).

Either during evolution (figure 5) or during post-evolutionary evaluations (figure 6), statistical results show that the CCNS model is clearly more efficient than the CC and NS models. Since their associated use is more salient than their individual application, we may conclude that there is a *synergy* between the two mechanisms.

In our model, the synaptic normalization is expressed in a static way. This assumption is made due to the fact that, from a biological point of view, this mechanism is relatively slow. However, it should be interesting to study its dynamic modelling as in Oja's learning rule (Oja, 1982). Moreover, by its local nature, this rule is more biologically plausible. In the same way, a dynamical regulation of neuron excitability could allows a wider range of dynamics.

Conclusion and further work

In this paper, we show that evolvabilty, in terms of both speed and final result, of plastic neural controllers is improved by couping them with bio-inspired homeostatic mechanisms that regulate neuronal excitability. Evolved controllers show increased stability and robustness. These results support the hypothesis that constraining neuronal architectures with homeostatic mechanisms at the micro-level induces robust behaviours at the macro-level (Di Paolo, 2002).

On the other hand, since our neuronal model is not specific to the task we test it on, our results suggest that these mechanisms could be beneficial to other applications or methodologies (back-propagation, reinforcement learning, *etc*). Indeed, in the case of back-propagation, the gradient descent on an error could include a multiplicative normalization mechanism of synaptic weights as in eq. (3). Moreover, the center-crossing mechanism should not need any adaptations to fit classical connexionism methods.

Within the scope of the IRON project, the aim of our current work is to extend our approach to robots of several morphologies undergoing various kind of perturbations. To this end, the addition of a dynamic system, driving intrinsic neuronal properties and synaptic plasticity, could improve neural controllers' adaptivity by allowing them to reconfigure themselves. A potential issue is to integrate to our neural model some bio-inspired paradigms based on chemical messengers (Eggenberger et al., 1999; Husbands et al., 1998).

References

Baker, J. E. (1987). Reducing bias and ineffiency in the selection algorithm. In Associates, L. E., editor, *Proc. of the second Int. Conf. on Genetic Algorithms and their Applications*, Hillsdale.

Beer, R. (1995). On the dynamics of small continuous-time recurrent neural networks. *Adaptive Behavior*, 3(4):469–509.

Desai, N., Rutherford, L., and Turrigiano, G. (1999). Plasticity in the intrinsic excitability of neocortical pyramidal neurons. *Nature Neuroscience*, 2(6):515–520.

Di Paolo, E. A. (2002). Fast homeostatic oscillators induce radical robustness in robot performance. In *SAB'2002*. MIT Press.

Dittrich, P., Buergel, A., and Banzhaf, W. (1998). Learning to move a robot with random morphology. In Husbands, P. and Meyer, J.-A., editors, *Evolutionary Robotics, First European Workshop, EvoRob98*, pages 165–178. Springer, Berlin.

Eggenberger, P., Ishiguro, A., Tokura, S., Kondo, T., and Uchikawa, Y. (1999). Toward seamless transfer from simulated to real worlds: A dynamically-rearranging neural network approach. In Wyatt, J. and Demiris, J., editors, *Proc. of the Eighth Eur. Workshop on Learning Robots*, pages 4–13, EPFL, Lausanne, Switzerland.

Floreano, D. and Urzelai, J. (1999). Evolution of neural controllers with adaptive synapses and compact genetic encoding. In *5th European Conf. on Artificial Life*.

Floreano, D. and Urzelai, J. (2000). Evolutionary robotics: The next generation. In Gomi, T., editor, *Evolutionary Robotics III*, Ontario (Canada). AAI Books.

Gallagher, J., Beer, R., Espenschied, K., and Quinn, R. (1996). Application of evolved locomotion controllers to a hexapod robot. *Robotics and Autonomous Systems*, 19:95–103.

Gerstner, W. and Kistler, W. (2002). *Spiking Neuron Models*, chapter 11. Cambridge Univ. Press. (`http://diwww.epfl.ch/~gerstner/BUCH.html`).

Goldberg, D. E. (1989). *Genetic algorithms in search, optimization, and machine learning*. Addison-Wesley, Reading, MA.

Hebb, D. (1949). *The Organization of Behavior: A Neurophysiological Theory*. John Wiley and Sons.

Husbands, P., Smith, T., Jakobi, N., and O'Shea, M. (1998). Better living through chemistry: Evolving gasnets for robot control. *Connection Science*, 10(3-4):185–210.

Ijspeert, A. J., Hallam, J. C. T., and Willshaw, D. J. (1998). From lampreys to salamanders: Evolving neural controllers for swimming and walking. In *From Animals to Animats: Proc. of the Fifth Int. Conf. of the The SAB*. MIT Press.

Mathayomchan, B. and Beer, R. (2002). Center-crossing recurrent neural networks for the evolution of rhythmic behavior. *Neural Computation*, 14:2043–2051.

Meyer, J.-A., Doncieux, S., Filliat, D., and Guillot, A. (2002). Biologically inspired robot behavior engineering. In Duro, R., Santos, J., and Graña, M., editors, *Evolutionary Approaches to Neural Control of Rolling, Walking, Swimming and Flying Animats or Robots*. Springer-Verlag.

Miller, K. and MacKay, D. (1994). The role of constraints in hebbian learning. *Neural Computation*, 6:100–126.

Nolfi, S. (1997). Evolving non-trivial behaviors on real robots: a garbage collecting robot. *Robotics and Autonomous System*, 22:187–198.

Oja, E. (1982). A simplified neuron model as a principal component analyzer. *Math. Biol.*, 15:267–273.

Turrigiano, G. (1999). Homeostatic plasticity in neuronal networks: the more things change, the more they stay the same. *Trends in Neuroscience*, 22(5):221–228.

Turrigiano, G., Leslie, K., Desai, N., Rutherford, L., and Nelson, S. (1998). Activity-dependent scaling of quantal amplitude in neocortical pyamidal neurons. *Nature*, 391:892–895.